Patient-Specific Design of Multi-Component Steerable Catheters

Phuong Toan Tran*, Alain Devreker*, Gabrijel Smoljkic*, Herbert De Praetere†, Paul Herijgers†,
Emmanuel Vander Poorten*, Jos Vander Sloten*
*Department of Mechanical Engineering, KU Leuven,
†Experimental Cardiac Surgery, University Hospital Leuven, Leuven, Belgium

***Abstract*—Catheter-based diagnostic and therapeutic interventions are gaining in popularity due to the limited invasive nature of the approach. This evolution persists despite limited visualisation and manoeuvrability of the catheter within the vasculature. 2D X-ray angiographic and fluoroscopic imaging methods expose patients to increased levels of radiation [1] and require injection of contrast agent prone to allergic reactions [2]. To overcome the absence of depth information, notable efforts are being conducted to fuse real-time 2D fluoroscopic images with pre-operatively reconstructed 3D models [3]. When deformations of the cardiovascular system occur due to physiological phenomema, the intervention, or due to the introduction of fairly stiff instruments, it becomes difficult to rely on pre-operative data. To overcome the abovementioned issues, CASCADE, a recent EU-funded FP7 project, investigates the development of *self-aware* robotic catheters. These steerable catheters embark several sensors to intra-operatively capture and reconstruct the vasculature *from within* the vessel. The development of such catheters is challenging, as the additional sensors should not interfere with the catheter's main diagnostic or therapeutic purpose. For trans-catheter aortic valve implantation (TAVI), the catheter should still be able to safely reach the implantation site to implant the replacement valve. Furthermore, since patients and implants differ, solutions should be patient-specific. This abstract presents a method to design patient-specific multi-component steerable catheters. Results suggest that for TAVI a pair of adequately-placed short 2-DoF actuators can substantially limit the interaction with the vasculature. Where the current approach is geometric, it should be expanded to better account for the dynamics of and the interaction with the cardiovascular system.**

I. Introduction

For the last decades, minimally invasive interventional techniques have been increasingly adopted all over the world. With smaller incisions and reduced tissue dissection, these procedures allow not only faster recovery and better patient satisfaction, but also treatment of patients that would be considered inoperable with classical surgery. However, due to the reduced field of view and restrained access to the patient's anatomy, minimally invasive approaches require alternative imaging systems and increased dexterity to appropriately control the instruments. In general, long learning curves are associated to these procedures. In particular, this is true for catheter-based endovascular procedures where conventional catheters provide very limited manoeuvrability and where fluoroscopic and echographic images give few insights about the location of the catheter within a dynamic and deformable vascular environment. Recent steerable catheter technology allows overcoming some of these limitations. Through internal actuation, these catheters can adapt the shape of their distal extremity [4]. However, also here safe operation relies on accurate visualization and registration of catheter pose relative to the environment. Research conducted within the CASCADE project departs from traditional fluoroscopic and echographic imaging and focuses on the integration of embedded sensors into steerable catheters, providing them with real time proprioceptive and exteroceptive senses. One of the challenges is to incorporate actuators and sensors while not interfering with the original diagnostic or therapeutic purpose.

In this paper, we present a method for designing multi-component steerable catheters for TAVI. TAVI treats stenosis of an aortic valve by implanting a stent-mounted bioprosthetic valve delivered on-site by a catheter. The latter is inserted through a vascular access site (e.g. the femoral artery) and guided up to the stenotic native valve where the implant is released [5]. The proposed approach allows patient-specific selection of a catheter configuration based on a geometric analysis of the interactions between the catheter distal extremity and the vascular environment.

In the remainder of this paper, section II describes the vessel and catheter models, as well as the developed optimization program. Section III presents the results of our simulations. Finally, section IV concludes this report by discussing directions for future developments.

II. Methods and Materials

A. Catheter Specifications

An envisioned catheter for efficient and safe TAVI integrates at its distal extremity a force sensor monitoring the interactions between the catheter distal tip and the vessel wall, a flow sensor for localisation of vessel branches, an intravascular ultrasound (IVUS) probe imaging successive aorta cross-sections during the procedure, and electromagnetic position sensors for registering the catheter position. Although several mechanisms for catheter steering have been developed in the past [4], the present work focuses on hydraulic McKibben actuators [6] with constant curvature deflection. Without loss of generality modules with 2 degrees of freedom (DoFs) to adjust the bending radius and the bending direction are considered. Table I presents typical dimensions used for the components of the envisioned catheter. McKibben actuators are enclosed by rigid spacers that serve as a base to attach the actuators to the catheter. Note that given their small dimensions, flow and position sensors are not modeled here.

TABLE I. DIMENSIONS AND MODELS OF CATHETER COMPONENTS

Component	Diameter[mm]	Length[mm]
Rigid cylinder		
Force sensor (EndoSense TactiCath)	2.5	20
IVUS (Volcano Visions PV 8.2F)	2.5	15
Position sensor (NDI Aurora 5DoF)	0.9	12
Valve (Edwards SAPIEN)	6	25
McKibben spacer	5	5
Section of torus		
Component	**Diameter[mm]**	**Length[mm]**
McKibben actuator	5	10 - 90
Rectangular plate		
Component	**Dimensions[mm]**	
Flow sensor (M7 Devices)	1.6×1×0.5	

The particular nature of TAVI and cardiovascular procedures in general constrains already the number of possible catheter configurations. To minimize surgical risks during TAVI, the catheter distal tip should ideally not intrude more than 50mm into the heart chamber when deploying the valve implant (in this first approach, this constraint is relaxed to 75mm). In addition, when using a force sensor, this must be placed at the very tip of the catheter, while the IVUS probe should be as close as possible to the tip. Given these constraints, possible configurations, starting from the catheter tip are:

Force sensor - IVUS - Valve - n McKibben (1)

Force sensor - IVUS - m McKibben - Valve - p McKibben (2)

with $m + p = n$, the number of 2-DoF McKibben modules.

B. Optimization Goal and Principle

The objective is now to determine the number, the length and the order of occurence of the McKibben actuators, so that minimal contact between the catheter and the vessel wall can be achieved while the former is being advanced along the vessel up to the heart chamber. All possible combinations of lengths according configurations (1), (2) and within the ranges of Table I are investigated. It is hypothesized that if at least theoretically (in the absence of gravity) the catheter can adopt a shape maximally coinciding with the center line, such configuration possesses excellent properties to also in reality limit the contact with the vasculature. In search for an ideal configuration we therefore solve for each configuration and for each place along the center line the actuation angles needed to maximally align both. At any point on this trajectory, if collisions between the catheter and the vessel wall occur, the penetration depth is evaluated. In combination with other design constraints, such as length and actuator bending radius, the penetration depth is used to compute an overall quality score for each configuration.

C. Aorta Model

A triangular surface mesh of the vessel wall is reconstructed using a CT scan provided by the Department of Radiology of the University Hospital. The center line is generated by taking the center of circles that approximate successive aorta cross-sections along the entire aorta. The resulting center line is resampled to obtain the desired resolution (Fig.1). Generation of the aorta mesh and center line is performed using Mimics (Materialise - Leuven, Belgium) and pyFormex [7].

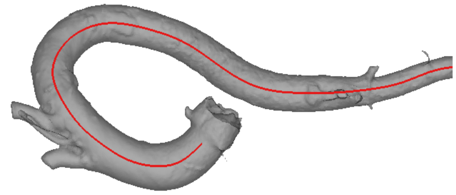

Fig. 1. Aorta mesh and center line (red) reconstructed from a CT scan.

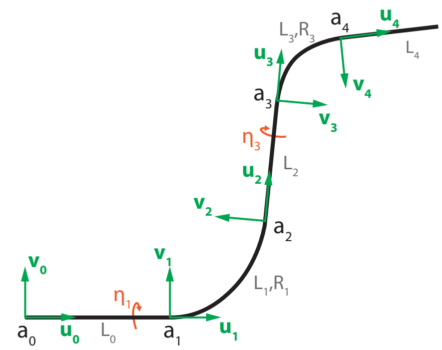

Fig. 2. Center line for catheter with 2 McKibben actuators. Part i of the catheter has a length L_i and is associated with a local reference frame $(\boldsymbol{u_i}, \boldsymbol{v_i}, \boldsymbol{n_i})$. Each actuator (here 1 and 3) possesses 2 DoFs: R_i and η_i.

D. Catheter Model

Two different representations of the catheter are used in the simulation. The catheter center line is used to simulate the catheter motion inside the aorta. A catheter mesh is used to detect and evaluate penetrations with the aorta.

1) Catheter Center Line: The catheter center line is modeled as a succession of line segments and circular arcs representing the different rigid components (sensors, McKibben spacer, valve) and the McKibben actuators respectively. This leads to a set of piece-wise parametrized vectorial equations of lines and circular arcs. Fig.2 shows the center line of a catheter with 2 McKibben actuators. Unit vectors $\boldsymbol{u_i}$ are defined such that each part of the center line is tangent to the previous one. Vectors $\boldsymbol{u_i}$ and $\boldsymbol{v_i}$ are orthogonal and form a plane in which the catheter part i lays. Together with $\boldsymbol{n_i} = \boldsymbol{u_i} \times \boldsymbol{v_i}$, they define a local reference frame on each part at $\boldsymbol{a_i}$. Each McKibben actuator has 2 DoFs: the bending radius R_i and the bending direction modeled by the angle η_i between $\boldsymbol{v_{i-1}}$ and $\boldsymbol{v_i}$. The angle η_i is the angle of rotation about vector $\boldsymbol{u_i}$.

2) Catheter Mesh: The catheter mesh is used to detect and evaluate collisions between the catheter and the vessel wall. Meshes of components described in Table I are obtained by folding a plane of triangular elements and closing the resulting surface with appropriate disks. Individual components are then automatically assembled using local frames defined at the extremities of each component. Parametric generation of such meshes is realized with pyFormex (Fig.3).

E. Catheter Motion

1) Optimization Program: Given one catheter configuration with n_{arcs} McKibben actuators, let $\boldsymbol{p_i}$ $(i = 0, \ldots, n-1)$ be n points of the catheter center line C_1, starting from the catheter proximal tip. $\boldsymbol{q_j}$ $(j = 0, \ldots, m-1)$ are m points of the aorta center line C_2, starting from the abdominal aorta

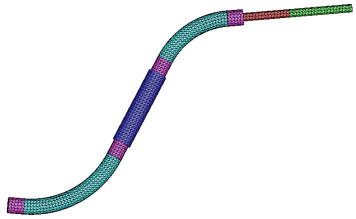

Fig. 3. Catheter mesh with force sensor (green), IVUS probe (red), valve implant (blue), McKibben spacers (magenta) and McKibben actuators (cyan).

to the heart valve. The proximal tip $\boldsymbol{p_0}$ of the catheter is fixed to a point $\boldsymbol{q_j} \in C_2$. The objective is then to find the transformation parameters to apply to C_1 to maximally fit C_1 to C_2. By finding these parameters for every point $\boldsymbol{q_j}$ of the aorta center line and applying these parameters to C_1, catheter motion along the aorta center line is simulated.

In total $3+2n_{arcs}$ DoFs are to be solved by this optimization problem, namely: 3 rotations about point $\boldsymbol{q_j}$ described by unit quaternion $z = (z_0\,; z_1\,; z_2\,; z_3)$ and transformation matrix $T(z)$; the change of the n_{arcs} radii R_k and n_{arcs} axial rotations η_k about the catheter center line. Let C_1' be the catheter center line after applying these transformations. By defining the distance between point $\boldsymbol{a}$ and curve C with points $\boldsymbol{b_j}$ as:

$$\mathrm{d_{min}}\left(\boldsymbol{a},\, C\right) = \min_j \|\boldsymbol{a} - \boldsymbol{b_j}\|, \tag{3}$$

a function F that must be minimized can be defined as the bidirectional point to curve mean squared distance:

$$\begin{aligned} F(z, R_k, \eta_k) = \frac{1}{2}\Bigg[& \frac{1}{n}\sum_{i=0}^{n-1} \mathrm{d_{min}}\Big(T(z)\boldsymbol{p_i}(R_k,\eta_k),\, C_{2,r}\Big)^2 \\ & + \frac{1}{t}\sum_{l=j}^{j+t-1} \mathrm{d_{min}}\Big(\boldsymbol{q_l},\, C_1'(z, R_k, \eta_k)\Big)^2 \Bigg] \end{aligned} \tag{4}$$

The aorta center line C_2 is restrained to the portion of interest $C_{2,r}$ containing t points from $\boldsymbol{q_j}$ to $\boldsymbol{q_{j+t-1}}$. The minimization of (4) is subject to the following constraints and boundaries:

$$\|z\| = 1 \tag{5}$$

$$T(z)\boldsymbol{u_0} \cdot (\boldsymbol{q_{j+1}} - \boldsymbol{q_j}) \geq 0 \tag{6}$$

$$-1 \leq z_i \leq 1 \text{ for } i = 0, \ldots, 3 \tag{7}$$

$$R_{min} \leq R_k \;(k = 2l+1 \text{ for } l = 0, \ldots, n_{arcs}-1) \tag{8}$$

$$-\pi < \eta_k \leq \pi \;(k = 2l+1 \text{ for } l = 0, \ldots, n_{arcs}-1) \tag{9}$$

Equation (6) constrains the first segment of C_1' to the local direction of C_2 at $\boldsymbol{q_j}$. R_{min} in (8) is defined as $R_{min}=\frac{L_k+\Delta}{2\pi}$ where L_k is the arc length and Δ=20mm.

2) Optimization Algorithm: The optimization program that minimizes objective function (4) under constraints (5-6) and within boundaries (7-9) is numerically solved within pyFormex with the sequential least squares programming (SLSQP) solver of the SciPy library [8], [9]. The initial guess required for such numerical solver is based either on a geometric analysis of the aorta center line shape or on the results of previous optimization steps. The set of initial parameters that allows achieving the minimal objective function value after optimization is used to determine the optimal parameter set.

TABLE II. CHARACTERISTICS OF MESHES AND CENTER LINES

	Aorta		**Catheter**	
	Mesh	**CenterLine**	**Mesh**	**CenterLine**
Resolution[mm]	0.97	3.97	1.09	2.15
Vertices	99556	113	1353-4396	37-125
Faces	199100	-	2916-9252	-
Length[mm]	-	445	-	80-260

F. Catheter Penetration Depth

For each point $\boldsymbol{q_j}$ on the aorta center line C_2, the catheter mesh is generated according to the result of the optimization program described in section II-E. Potential collisions with the aorta are detected and evaluated using ray tracing algorithms based on the Jordan curve theorem [10], [11] and Kd-tree nearest neighbors [12]. For our purpose of comparing different catheter configurations in a vessel with relatively limited tortuosity, the penetration depth $d_{p,j}$ of the catheter inside the aorta wall for position $\boldsymbol{q_j}$ can be defined as

$$d_{p,j} = \sum_{h=0}^{n_{out,j}-1} \min_g \left\|\boldsymbol{m_{cath,h}} - \boldsymbol{m_{aorta,g}}\right\|^2 \tag{10}$$

with $\boldsymbol{m_{cath,h}}$ $(h = 0, \ldots, n_{out,j}-1)$ the location of the $n_{out,j}$ vertices of the catheter mesh that lie outside the aorta for the simulated step $\boldsymbol{q_j}$ and with $\boldsymbol{m_{aorta,g}}$ the locations of the vertices of the aorta mesh.

G. Characterization of Catheter Configurations

By defining $d_p^{ci} = \sqrt{\sum_j d_{p,j}}$ and $\theta^{ci} = \max_k \frac{L_k}{R_{k,min}}$, each configuration ci is characterized by a score

$$S^{ci} = \alpha\frac{d_p^{ci}}{\max_{ci} d_p^{ci}} + \beta\frac{\theta^{ci}}{\max_{ci}\theta^{ci}} \tag{11}$$

The lower the score, the better the configuration is. The α-term relates to the amount of collisions that the catheter produces when following the aorta center line. The β-term accounts for the design constraints of the actuators. Shorter length L_k of actuators k allows easier local position control. On the other hand it is harder to manufacture actuators k that can generate a very small bending radius $R_{k,min}$.

III. Results

Fig.4 compares the scores obtained for each catheter configuration. For this evaluation, α and β were set to $\alpha = 0.7$ and $\beta = 0.3$, putting thus a relative high weight β on ease of manufacturing. A maximum of 2 McKibben actuators is considered. Their respective length varies from 10 to 90mm with a 10mm step. Following the catheter specifications described in section II-A, 110 different configurations are compared. Characteristics of meshes and center lines generated during the simulations are presented in Table II. The resolution is the mean distance between adjacent vertices. The vessel center line is restricted from the abdominal aorta to the aortic valve. Simulations are performed on a PC with 2 Intel Xeon CPU E5-2620 @ 2.00GHz and 32GB RAM. The total computation time was about 110 hours (thus about 1 hour per configuration). We expect that there are still substantial opportunities to further speed up the current implementation. Collisions between

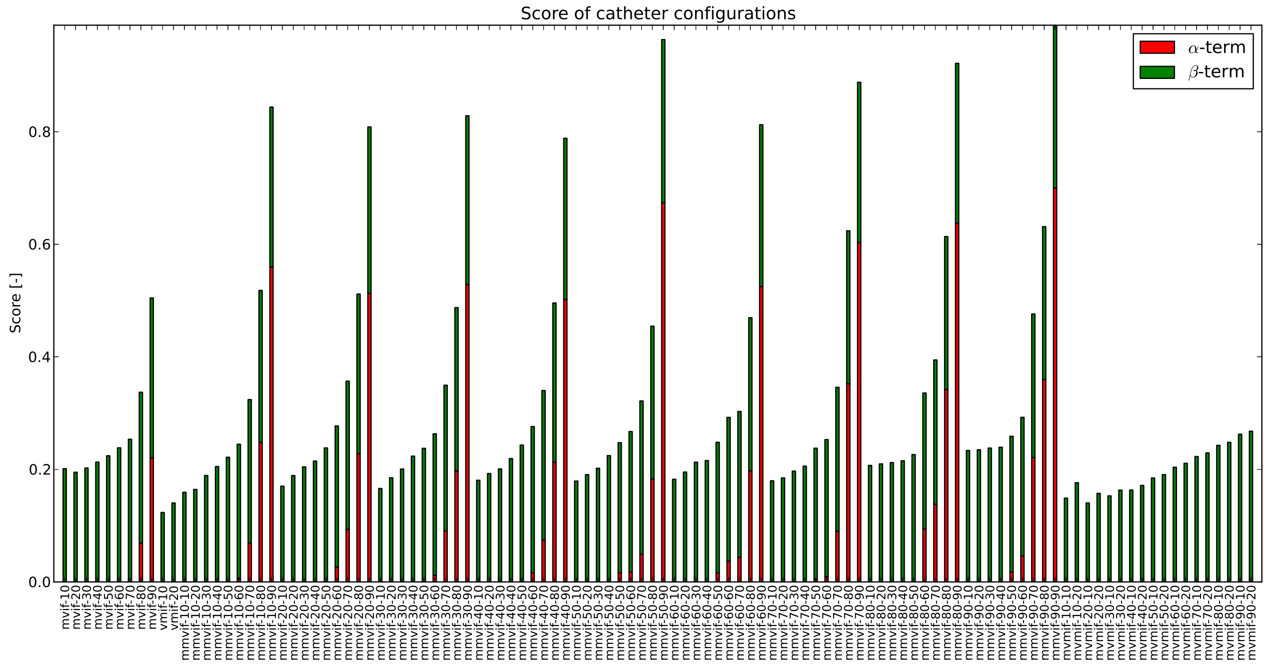

Fig. 4. Score of each catheter configuration. Each configuration is identified by an acronym stating which components are in the catheter (m: actuator, v: valve, i: IVUS sensor, f: force sensor), the relative order (from proximal part to distal tip), and the actuator length (from proximal part to distal tip) in mm.

catheter and vasculature occur when the actuator length limits the catheter manoeuvrability. This occurs when there is no actuator between valve and sensors. Such an actuator would allow better controllability since rigid parts of the catheter are shorter and can be steered more efficiently to avoid contact. The required bending angle generally increases with actuator length, since longer actuators have to bend more to follow the aorta center line, especially in the region of the aortic arch. These results thus suggest that an optimal catheter configuration for TAVI should include short actuators adequately located to deal with the rigid parts of the catheter.

IV. Conclusion

This paper describes a first approach to design multi-component steerable catheters comprising 2-DoF actuators with constant curvature deflection. Current simulation results favor adequately placed short actuators. However, the results are based on a pure geometric analysis, assuming that the catheter's proximal part always lays on the aorta center line. A simulation incorporating the mechanical properties of the catheter, such as described in [13], and more efficient and precise collision detection would allow better estimates of the contact and interactions with the vessel. Although illustrated for TAVI, the presented method can be applied to other procedures that would benefit from multi-component catheters.

Acknowledgment

This research was supported by the EU's Seventh Framework Programme under GA No. 601021 (CASCADE).

References

[1] I. Pantos, G. Patatoukas, D. Katritsis, and E. Efstathopoulos, "Patient radiation doses in interventional cardiology procedures," *Current Cardiology Reviews*, vol. 5, no. 1, pp. 5–11, 2009.

[2] M. Saljoughian, "Intraveous radiocontrast media: A review of allergic reactions," *US Pharmacist*, vol. 37, no. 5, pp. 14–16, 2012.

[3] S. Liao, R. Miao and Z. Y., "Automatic and efficient contrast-based 2-d/3-d fusion for trans-catheter aortic valve implantation (tavi)," *Computerized*, vol. 37, pp. 150–161, 2013.

[4] Y. Fu, H. Liu, W. Huang, S. Wang, and Z. Liang, "Steerable catheters in minimally invasive vascular surgery," *The International Journal of Medical Robotics and Computer Assisted Surgery*, vol. 5, no. 4, pp. 381–391, Jul. 2009.

[5] C. R. Smith, M. B. Leon, M. J. Mack, D. C. Miller, J. W. Moses, L. G. Svensson, E. M. Tuzcu, J. G. Webb, G. P. Fontana, R. R. Makkar *et al.*, "Transcatheter versus surgical aortic-valve replacement in high-risk patients," *New England Journal of Medicine*, vol. 364, no. 23, pp. 2187–2198, Jun. 2011.

[6] A. Moers, M. De Volder, and D. Reynaerts, "Integrated high pressure microhydraulic actuation and control for surgical instruments," *Biomedical Microdevices*, vol. 14, no. 4, pp. 699–708, Aug. 2012.

[7] B. Verhegghe. pyFormex Homepage. [Online]. Available: http://www.nongnu.org/pyformex/

[8] D. Kraft, "A software package for sequential quadratic programming," DLR German Aerospace Center – Institute for Flight Mechanics, Koln, Tech. Rep. DFVLR-FB 88-28, 1988.

[9] E. Jones, T. Oliphant, P. Peterson *et al.* (2001) SciPy: Open source scientific tools for python. [Online]. Available: http://scipy.org/

[10] J. O'Rourke, *Computational geometry in C.* Cambridge university press, 1998.

[11] C. J. Ogayar, R. J. Segura, and F. R. Feito, "Point in solid strategies," *Computers & Graphics*, vol. 29, no. 4, pp. 616–624, Aug. 2005.

[12] J. L. Bentley, "Multidimensional binary search trees used for associative searching," *Communications of the ACM*, vol. 18, no. 9, pp. 509–517, Sep. 1975.

[13] T. Alderliesten, M. K. Konings, and W. J. Niessen, "Modeling friction, intrinsic curvature, and rotation of guide wires for simulation of minimally invasive vascular internventions," *Biomedical Engineering, IEEE Transactions on*, vol. 54, no. 1, pp. 29–38, Jan. 2007.